



TWO DIMENSIONAL NUMERICAL MODELING OF FLOW IN TRAPEZOIDAL BEND CHANNEL USING SPUR DIKE

Saleh I. Khassaf¹ and Samiya Ghaffar Saeed²

1 Professor, Department of Civil, Faculty of Engineering, University of Basrah,
alkhssafmustafa@yahoo.com

2 Directorate General of Education in Al-najaf Al-ashraf, Ministry of education,
sameng62@yahoo.com

ABSTRACT

A two-dimensional hydraulic flow model was developed using the SMS software (Surface Water Modeling System) to simulate the flow properties (thalweg line location) for meander in trapezoidal section channel, and its changes when a single emerge spur dike install at mid of the bend. The model was calibrated and verified through matching velocity profiles throughout the study reach.

Thalweg line location were found due to the variation of spur dike characteristic including 180 runs, included five different ratios of spur dike length to top channel width (L/T_w), five ratios of spur dike arm to its body length (l/L), and two spur arm's direction for four different flow rates, as a result, through the flow configuration the new location of the thalweg in the bend channel after using the spur dike was about (44-71)% T_w which mainly affected by spur body length.

KEY WORDS

Single Spur Dike, Thalweg Line Meandering Channel, Numerical Models, Velocity Distribution.

النموذج العددي للجريان في قناة منحنية مع استعمال مسنة مفردة

أ.د. صالح عيسى خصاصف

سامية غفار سعيد

جامعة البصرة، كلية الهندسة، قسم الهندسة
المدنية

وزارة التربية، المديرية العامة للتربية في
النجف الاشرف

الخلاصة

أستخدم البرنامج الجاهز (SMS) لتطوير موديل هيدروليكي ثنائي البعد ولتمثيل خصائص الجريان (موقع خط التالوك) لمنحني ذو مقطع شبه منحرف، وتغيراته بعد وضع مسنة في منتصف المنحني، تمت معايرة النموذج وعملية التحقق للبرنامج من خلال عمليات مقارنة لقيم السرعة. وجد موقع خط التالوك تبعاً لتغير خصائص المسنة، حيث اجريت 180 تجربة متضمنة تغير في نسبة طول جسم المسنة (L/T_w)، نسبة طول ذراع المسنة (l/L)، اتجاه ذراع المسنة وتحت تأثير اربعة تصاريح مختلفة و وجد ان موقع خط التالوك يتراوح بين (44-71)% من عرض سطح القناة، متأثراً وبشكل أساسي بطول جسم المسنة.

1. INTRODUCTION

Meander in rivers is the most common and important river pattern because of complicated flow that affect by the centrifugal force which acting on the flow around bends, and producing an unique features affects the stability river, which represented by Superelevation, Transverse current, and Maximum-velocity current lead to degradation of channel beds, erosion on channel banks, and bend migration. Meander geometry and there complex flow pattern amplifies the challenges of control and alteration for river, so it important to understand natural river flow patterns and their processes to apply this information to projects involving the alteration [1]. A number of measures exist that may be taken to assist the achievement of a control and alteration reach. Three general classifications of bank stabilization techniques including: armor protection, indirect protection, and bio-engineering. Each technique has specific advantages and disadvantages, but there are no specific guidelines stating which stabilization type is most suitable for a specific situation [2]. Spur dike is one of the indirect protection mean identified as appropriate structures to potentially protect the natural habitat and produce the vulnerable river banks, its have become a relatively inexpensive method of achieving multiple stream restoration goals, because these native material structures, and are constructed of easily accessible materials [3]. In this study, the 2-D numerical model was developed to study the flow pattern in meander bend channel and the effects of use single emerge spur dike, adopting different size and head shape, and measure the hydraulic characteristics to locate the position of the *thalweg line*, which is *refer to the line of the maximum flow velocity* which has the deepest portion of the river causes from scour action that affected by the high velocity.

2. NUMERICAL MODEL

SMS/RMA2 modeling package is a two-dimensional depth averaged finite element hydrodynamic numerical model. RMA2 solves the depth-integrated equations of fluid mass and momentum conservation in two horizontal directions, with take the secondary flow effect, the program solves a transport equation for stream wise vorticity and converts it to accelerations due to secondary currents. The inclusion of these additional accelerations results in improved predictions of depth-averaged velocity in bends flow, in particular, their effect (accelerations due to secondary currents) is to reduce depth-averaged velocities on the inside of curves and increase them on the outside of curves [4]. The forms of these equations are:

$$\frac{\partial h}{\partial t} + h \left(\frac{\partial \bar{u}}{\partial x} + \frac{\partial \bar{v}}{\partial y} \right) + \bar{u} \frac{\partial h}{\partial x} + \bar{v} \frac{\partial h}{\partial y} = 0 \quad (1)$$

$$h \frac{\partial \bar{u}}{\partial t} + h \bar{u} \frac{\partial \bar{u}}{\partial x} + h \bar{v} \frac{\partial \bar{u}}{\partial y} - \frac{h}{\rho} \left(\varepsilon_{xx} \frac{\partial^2 \bar{u}}{\partial x^2} + \varepsilon_{xy} \frac{\partial^2 \bar{u}}{\partial y^2} \right) + h g_x \frac{\partial a}{\partial x} + h g_y \frac{\partial h}{\partial x} - \tau_y + S_x = 0 \quad (2)$$

$$h \frac{\partial \bar{v}}{\partial t} + h \bar{u} \frac{\partial \bar{v}}{\partial x} + h \bar{v} \frac{\partial \bar{v}}{\partial y} - \frac{h}{\rho} \left(\varepsilon_{xx} \frac{\partial^2 \bar{v}}{\partial x^2} + \varepsilon_{xy} \frac{\partial^2 \bar{v}}{\partial y^2} \right) + g h \left(\frac{\partial a}{\partial x} + \frac{\partial h}{\partial y} \right) - \tau_x + S_y = 0 \quad (3)$$

Where

h = depth, \bar{u}, \bar{v} = depth-averaged velocities in the Cartesian directions, x, y, t = Cartesian coordinates and time, ρ = density of fluid,

ε = eddy viscosity parameter, for xx = normal direction on x axis surface, for yy = normal direction on y axis surface, for xy and yx = shear direction on each surface,

g = acceleration due to gravity, a = elevation of channel, n = Manning's n parameter quantifying roughness characteristics, 1.486 = conversion from SI (metric) to English units,

S_x and S_y = accelerations that result from the non uniformity of u and v in the vertical direction, that is,; and τ_x , τ_y = external traction (bottom friction, wind, and Coriolis effects).

3. MODELING APPROACH

The bend of meandering channel that presented in this research was a concrete channel had relative curvature (R_c/T_w) 2.02 and its bend angel is (125°). The cross-sectional geometry was trapezoidal with a 1V:3H side slope and total channel depth was (0.46 m). Bed width is (5.85 m) [5] Fig.1 illustrate the bend schemes adopted in the study.

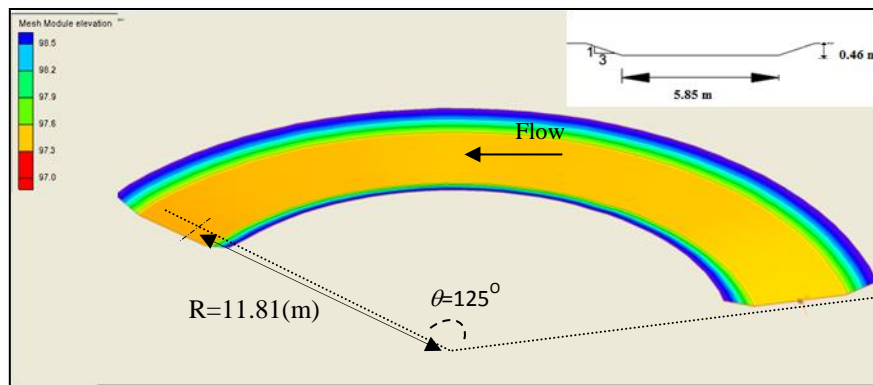


Fig. 1. Bend Channel Shape [5]

Modeling approach of a hydrodynamic model refers to the process of creating input files that describe the geometry, bathymetry, hydraulic characteristic, and boundary conditions of the meandering channel bend for simulation by use of the generalized hydrodynamic model RMA2. Defining the size and the shape of the finite elements could be controlled to create a suitable model and define material properties like channel roughness and eddy viscosity to had similar hydraulic properties [6].

Initially all elements were assigned with constant Manning's (n); the initial value should be within the plausible range. This value was modified during the calibration process to improve the match between field data and model program results.

In addition to channel roughness, each element was initially assigned with a starting value of eddy viscosity (E). Eddy viscosity controls both the stability of the numerical solution and the distribution of velocities across the channel. Values of eddy viscosity that are too small allow changes in the direction of velocity vectors that are too great for the numerical solution to converge. Thus, a minimum value of eddy viscosity was required to achieve numerical stability.

Eddy viscosities were reassigned based on the assigned Peclet number equation (4); The Peclet number dynamically adjusts the value of (E) after each model iteration based on the computed velocity, size, and fluid density of each element [7],[8].

$$E = \frac{\rho \cdot u \cdot dx}{P_e} \quad (4)$$

Where

P_e =Peclet number, ρ = fluid density, u = average elemental velocity, dx =length of the element in streamwise direction, And E =eddy viscosity.

Boundary conditions were set once the mesh had been created, and evaluated, and material properties have been assigned. In RMA2, a water surface elevation was specified for the outflow boundary and discharge to the model was specified at inflow boundaries [8].

4. CALIBRATION AND VALIDATION

Finite element models are simplified, discrete representations of complex and continuous physical flow systems. Three-dimensional topographic features are represented by two-dimensional elements, and the physics of flow are considered to obey differential equations in which several empirical coefficients appear. When a model produces useful results, they need to be calibrated if enough data are available. Model calibration is the process of adjusting the dimensions of simplified geometric elements and empirical hydraulic coefficients so that values computed by a model reproduce as closely as possible measured values [9].

In this study model calibration and validation included matching velocity magnitude profiles at cross sections throughout the study reach, which served by Heintz (2002), [5], and consider the Manning's N Values and Peclet number as main empirical coefficients [8].

Calibration process included using one flow condition ($0.57\text{m}^3/\text{s}$). An additional flow conditions then were simulated without changing the computational mesh or model parameters, and the simulated values were compared with measured velocities in the field to validate the model. The results of calibration process were a multi material assignment of roughness in the bend, where divide to two zones, main and sides. Bend sides divided to inside of bend which represented the convex, and outside bend represented the concave, as shown in Fig. 2, this method gives best match with average of error percent (7.3%). Finally Manning's value for channel shown in Table 1 with constant Peclet number for all elements equal 20.

Table 1. Manning's N Values for Each Zone

Inner zone	Middle zone	Out zone
0.012	0.011	0.014

Validation process is verifying the calibration results by applying additional flow conditions, which simulated without changing the computational mesh or model parameters from calibration process, the results of Validation process for the average error of (7.8%).

Depending on the calibration and the validation, it could be considered that the hydrodynamic model simulation was adequate; therefore the model results will be adopted.

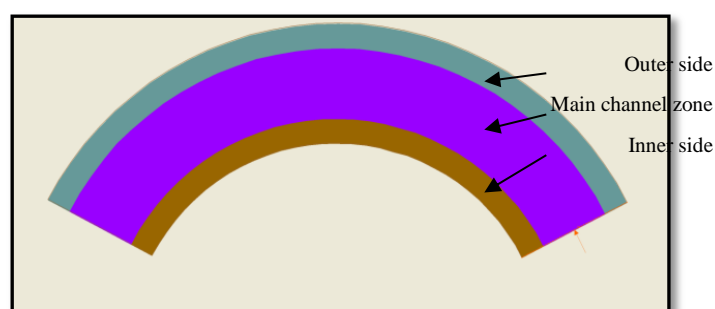


Fig. 2. Multi material define for the bend

5. VELOCITY DISTRIBUTION RESULTS OF CHANNEL BEND USING NUMERICAL SOLUTION AND THALWEG LINE LOCATION

After calibration and verification of the RMA2 simulation models, the two dimensional depth-averaged velocity predictions were found with RMA2 as velocity distribution maps presented in Figs. 3 and 4, where generally the higher velocities occur towards the outer bank starting from the beginning of the bend and continuing to the bend exit (because the effects of

centrifuge force), depended on these maps its could locate the thalweg line which is refer the line of the maximum flow velocity that has the deepest portion of the river.

Thalweg location in the bend channel varies with flow rate change, for lower flows (0.23 and 0.34 m^3/s), the pattern as shown in Fig.3 the same, thalweg line is about in center line of channel in the first sections and moves with small value toward the outer bank side, to reach $Tcl=44%$ and $Tcl=40%$ from top channel width (T_w) at the bend end), where Tcl measured at the bend end and with respect to outer bank side for (0.23 and 0.34 m^3/s) respectively.

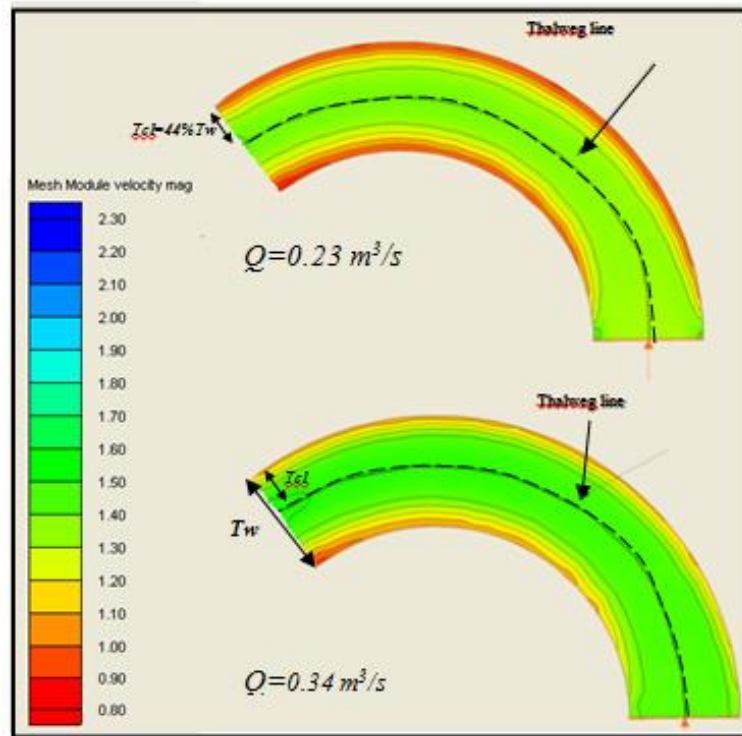


Fig. 3. Thalweg Line Location (0.23 m^3/s and 0.34 m^3/s)

In higher flow rate (0.45 and 0.57 m^3/s) fig 4, thalweg line location is approaching to the outer bank and along the upstream bend, the thalweg line location was $Tcl=23%$ and $Tcl=18%$ from top channel width (T_w), where Tcl measured at the bend end and with respect to outer bank side.

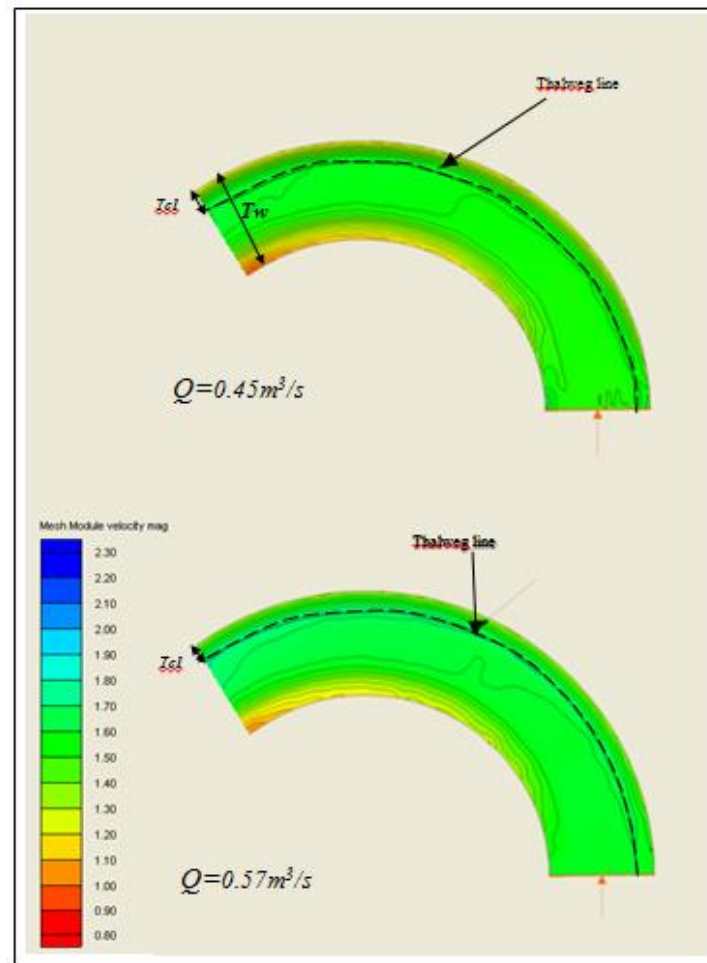


Fig. 4. Thalweg line location ($=0.45\text{m}^3/\text{s}$ and $0.57\text{m}^3/\text{s}$)

A thorough understanding of flow properties through channel bend leads to an understanding of erosion patterns. High velocity line location (thalweg line) important role in the processes of erosion and deposition, where the thalweg line in the outer bank causes erodes material from the outer bank and deposits material along the inner bank, forming point bars, constriction of bends due to the formation of point bars enables erosion to continue, allowing the meandering streams to migrate both in lateral and longitudinal directions.

6. USING SINGLE EMERGE SPUR DIKE

Spur dikes are hydraulic structures that project from the bank of a stream at some angle to the main flow direction. They are used for two purposes, namely river training and erosion protection of the riverbank. Spur dikes may be built as a single structure, namely a single spur dike, or as a series of spur dikes built in a row, along one or both sides of a river [11]. The primary objective from using the spur dike is to move the thalweg from its position along an eroding bank to a more favorable alignment (shifts toward the center of the channel), [12], [13], and re-distributes available energy within the project reach and dose not transfer it down stream [14].

In this study 180 simulations models were proposed with varying spur dike properties, which placed in the mid of the bend channel model, three cases were used to measure the characteristics changes in the flow field (thalweg line location), which concluded:

- 1) The spur dike body length change $L = (0.1, 0.16, 0.22, 0.28, 0.33)T_w$.
- 2) The extended spur dike arm's length change $l = (0, 0.25, 0.5, 0.75, 1) L$

3) The arm direct with respect to spur body were taken (90 degree) or upward L shape (opposite the flow) and (270 degree) or downward L (with flow) as shown in Fig.5. All these cases were applied under four different flow rates $0.23\text{m}^3/\text{s}$, $0.34\text{m}^3/\text{s}$, $0.45\text{m}^3/\text{s}$ and $0.57\text{m}^3/\text{s}$, however, all other properties constant.

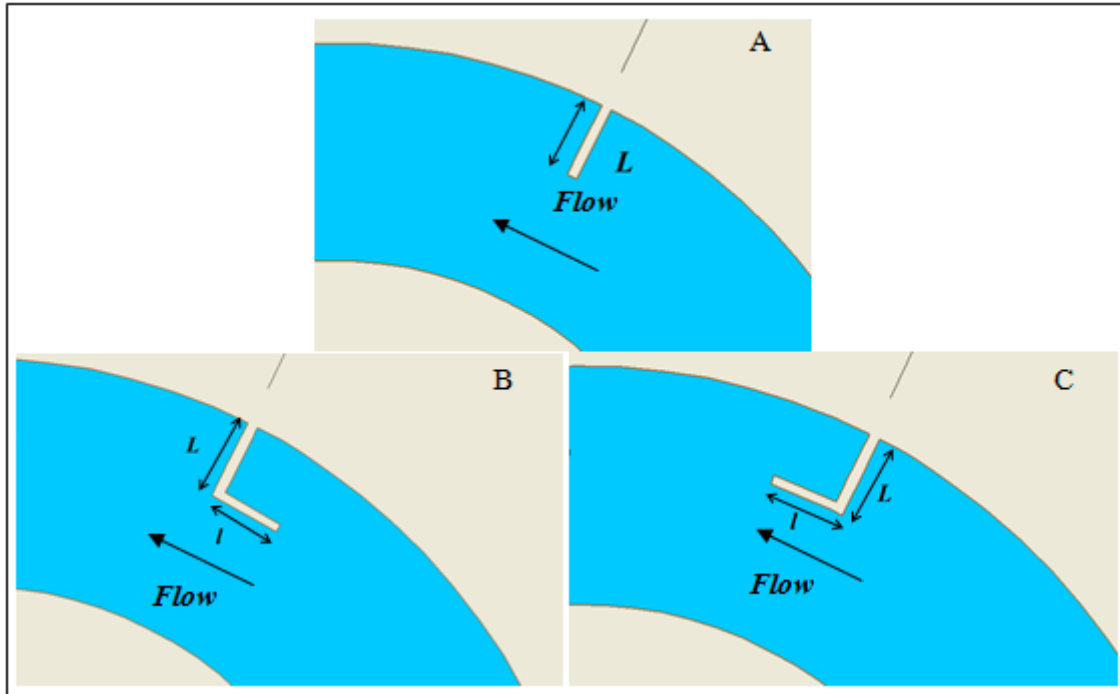


Fig. 5. Spur Dike Shape , A: Straight Spur Dike , B: Up Ward Spur $\theta=90^\circ$, C: Down Ward Spur $\theta=270^\circ$

7. RESULTS OF USING SINGLE SPUR ON FLOW CHARACTERISTICS (THALWEG LINE LOCATIONS)

Thalweg line location after using the spur dike was shifted toward the inner bank of the channel as shown in Fig. 6, the body length of spur dike has direct influence on the thalweg line location, where by increasing body length of the spur dike the thalweg line location from the outer bank (Tcl) increases. The increase pattern is a proximally linear and the impact is mainly within the scope of 44% - 71% of the top channel width (Tw) as shown in Fig. 7.

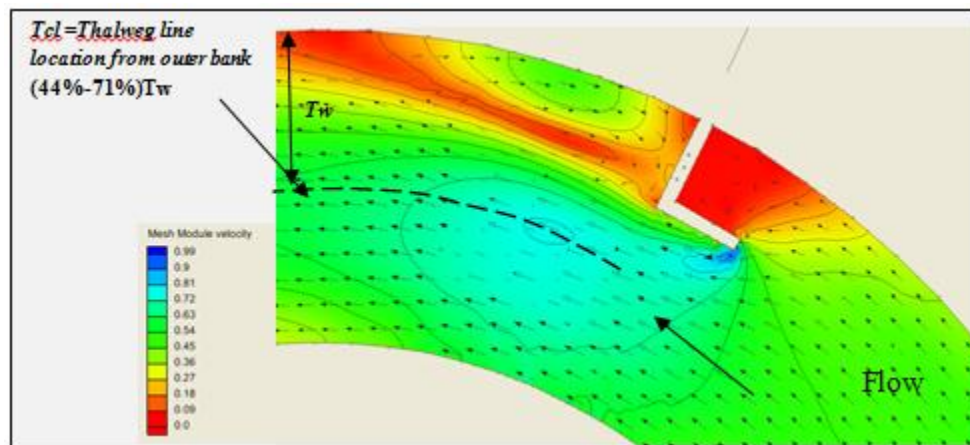


Fig. 6. Thalweg Line Location After Installed the Spur Dike ($Q=0.57\text{m}^3/\text{s}$)

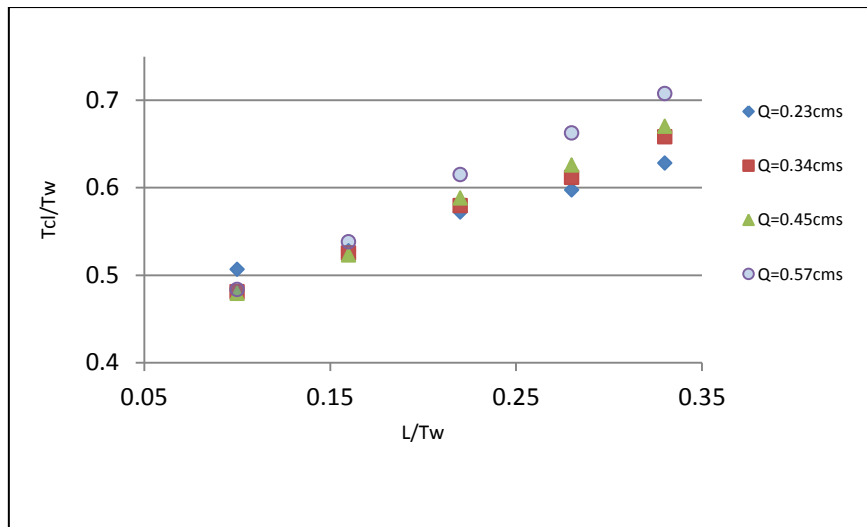


Fig.7. Effect of Body Length on Thalweg Height Tcl for ($l=0.75L$, $\theta=270^\circ$)

The change of the extended arm length had no great impact on the thalweg. Nonetheless, there are some of adverse trend, as shown in Fig. 8.

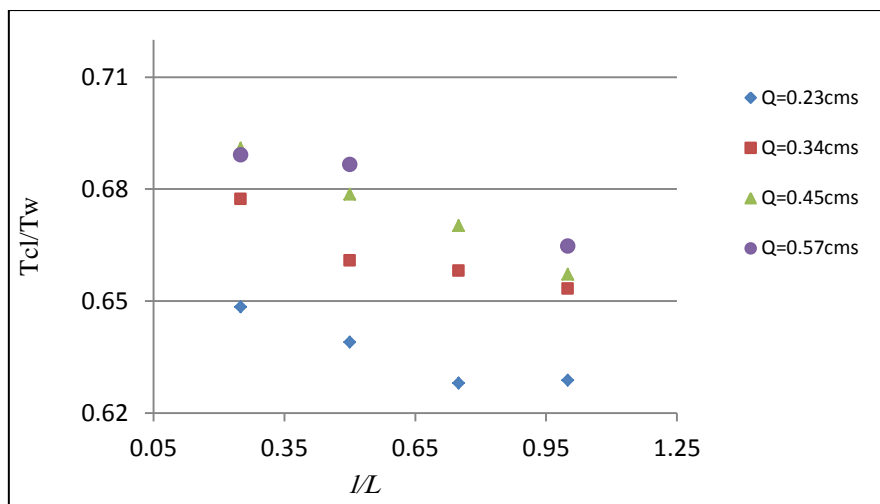


Fig. 8. Effect Of Spur Dike Arm Length Ratio (l/L) on The Thalweg Height Ratio (Tcl/Tw) for ($L=0.33Tw$, $\theta=270^\circ$).

Arm direction effects was variable with L/Tw change, for low body length ratio ($L/Tw=0.1$), thalweg line location (Tcl/Tw) for $\theta=90^\circ$ is greater than $\theta=270^\circ$, but for high body length ratio ($L/Tw=0.22$, 0.28 and 0.33), (Tcl/Tw) for $\theta=270^\circ$ is greater than $\theta=90^\circ$. as shown in Fig. 9.

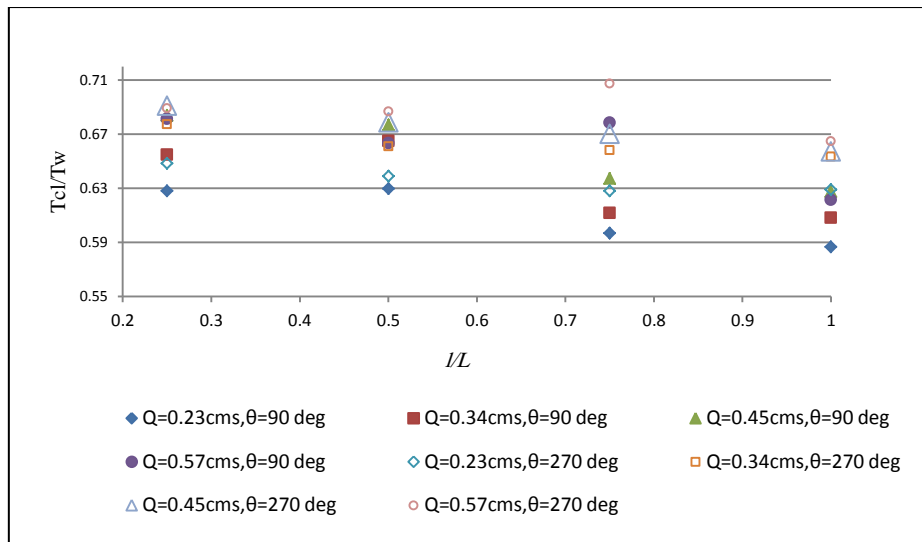


Fig. 9. Effect of Arm Direct of Spur Dike on The Thalweg line Location Ratio (Tcl/Tw), (L/Tw = 0.33)

Flow rate change were represented by Froude number, which considered as the average value at the iteration part of the bend channel, the results show that the impacts of Fr on the thalweg line location (Tcl/Tw) were differently and can be divided into two parts depend on the change in body length (L/Tw), where for high value (L/Tw=0.22, 0.28 and 0.33) the effect was direct, where thalweg location (Tcl/Tw) by increases in Fr, and for lower body length (L/Tw=0.1 and 0.16), Froude number effect is adversely on the thalweg height, thalweg height decreases when Fr increases as shown Fig.10.

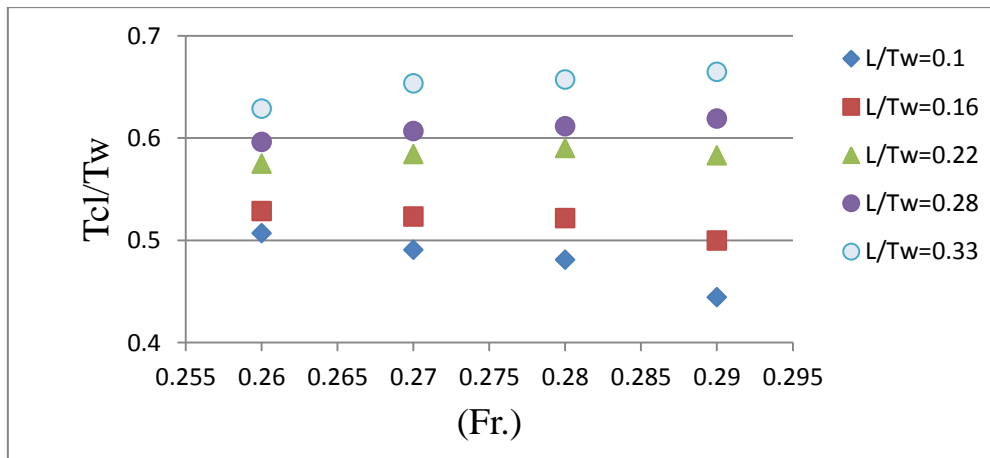


Fig.10: Effect of Froude number on the thalweg height ratio (Tcl/Tw) (L/Tw=0.33, theta=270°)

8. CONCLUSIONS

This study deal with flow pattern in a trapezoidal bend channel under various discharges, the channel was numerically simulated using a two-dimensional model by using SMS/RMA2 software. The numerical model was simulated with two cases, with and without using spur dike. Thalweg line location was found depended on the velocity distribution maps.

In first case (bend channel without using spur dike), The location of thalweg and flow pattern vary with discharge, where the thalweg line location was close to the outer bank side, with flow rate increase thalweg, line location was closer to outer bank because of increases in the flow force; thalweg location from outer bank was about (0.18-0.44) Tw, the eroding area in

various flow rates is in the outer bank side and become closer as flow rate increase to reach $0.18T_w$ (e.g. erodes line position at the outer bank).

When the spur dike is used as protection mean, it is very effective to shifted the thalweg line (eroding area) location from outer part to the inner part, where the new location of the thalweg location in bend channel after using the spur dike was about $(44-71)\%T_w$ which mainly affected by spur body length, while arm length wasn't effective. Arm direct effects was varying with body length change, where, for low body length ratio $\theta=90\text{deg}$ had the greater effect, but $\theta=270\text{deg}$ more effective for higher body length. The effect of (Fr) change (e.g flow rate change) on the thalweg line location were different and can be divided into two parts depend on the change in body length (L/T_w) , where for high value $(L/T_w=0.22, 0.28\text{ and } 0.33)$ the effect was direct, while Froude number effect was adversely at lower body length $(L/T_w=0.1\text{ and } 0.16)$; that's mean high flow rate river cases needed high value of body length to protect river from erosion, or else the low body length may causes more erosion, when the discharge increase.

9. REFERENCES

- [1] MacBroom J.G., (1981), "Factors affecting the stability of structures erected along water courses", Report No.31, The University of Connecticut, Institute Of Water Resources.
- [2] Darrow J.D., (2004), " Effects of bendway weir characteristics on resulting flow conditions", M.S. Thesis, Colorado State University, Fort Collins, CO.
- [3] Biedenharn D. S., Elliott C. M, and Watson C. C., (1997), " The WES stream investigation and stream bank stabilization hand book", (EPA) U.S. Army Engineer Waterways Experiment Station (WES)
- [4] Finnie et al., (1999), "Secondary flow correction for depth-average flow calculations", Journal of Engineering Mechanics, ASCE, 125(7), 848-863.
- [5] Heintz, M.L. (2002). "Investigation of bendway weir spacing", M.S. Thesis, Colorado State University, Department of Civil Engineering, Fort Collins, CO.
- [6] Stewart, G.B., (2000), "Two-dimensional hydraulic modeling for making instream-flow recommendations", M.S. Thesis, Colorado State University, Department of Civil Engineering, Fort Collins, CO.
- [7] Holtschlagd D.J. and Koshik J.A.(2002). " A two-dimensional hydrodynamic model of the St. Clair–Detroit river waterway in the Great Lakes Basin", Water-Resources Investigations Report 01-4236, Detroit District, U.S. Army Corps of Engineers.
- [8] Donnell B.P., Finnie, J.I., Letter, J.V., Jr., Mc Anally, W.H., Roig, L.C., and Thomas, W.A., (2003), Users guide to RMA2 WES Version 4.5: U.S. Army Corps of Engineers Waterway Experiment Station.
- [9] David C. Froehlich, (2002), User's Manual for FESWMS Flo2DH Two-dimensional Depth-averaged Flow and Sediment Transport: FHWA, , Virginia 22101
- [10] Azinfar H., (2010), "Flow resistance and associated backwater effect due to spur dikes in open channels", PhD Thesis, University of Saskatchewan.
- [11] Brown S.A.,(1985), " Design of spur-type stream bank stabilization structures", FHWA/RD-84/101, McLean, Virginia

- [12] Rhoads B.L., (2003), "Protocols for geomorphic characterization of meander bends in Illinois", Department of geography, university of ILLINOIS at URBANA-CHAMPAIGN URBANA, IL 61801
- [13] Dishman D. R., (2005), "Design of stream barbs", Version 2.0, Engineering Technical note NO. 23, NRCS.

LIST OF SYMBOLS

Symbol	Definition	Dimensions
Θ	Arm spur dike angle	Rad.
ρ	Density	M/L^3
A	Bottom elevation	L
B	River bed width	L
BW	Channel Bottom Width	L
D	Depth	L
E	Eddy viscosity	L^2/T
Fr	Froude number	-
G	Specific weight	M/T^2
H	Depth	L
L	Body spur dike length	L
L	Arm spur dike length	L
N	Manning's roughness coefficient	-
\mathbf{N}	Unit vector normal to u	-
Pe	Peclet number	-
Q	Volumetric Flow Rate	L^3/T
R	Bend Radius	
Rc	Bend Relative Curvature (R/B)	-
$RMA2$	Model developed by <u>R</u> esource <u>M</u> anagement <u>A</u> ssociates with US Army Corps of Engineers (USACE)	
S	Acceleration arising from secondary flow	-
SMS	<u>S</u> urface water <u>M</u> odeling <u>S</u> ystem	-
S_o	Bed Slope	-
T	Time	T
Tw	Top surface width	L
U	x-component of velocity	L/T
u^-	Depth-averaged u velocity	L/T
V	y-component of velocity	L/T
v^-	Depth-averaged v velocity	L/T
V_{app}	Velocity in inflow channel part	L/T
$V_{max}(levee)$	The maximum velocity near channel levee	L/T
$V_{max}(main)$	The maximum velocity in main channel	L/T
W	River width	L
Z_b	Bottom elevation	L
Z_s	The elevation of free surface	L